Official English translation

AUTOMODULATION AND CHAOTIC REGIMES OF GENERATION IN A TWO-RESONATOR GYROKLYSTRON WITH DELAYED FEEDBACK

R. M. Rozental[1], *O. B. Isaeva*[2], *N. S. Ginzburg*[1], *I. V. Zotova*[1], *A. S. Sergeev*[1], *A. G. Rozhnev*[2], *V. P. Tarakanov*[3,4]

[1]Federal Research Center The Institute of Applied Physics of RAS
46, Ul'yanova str., Box-120, 603950 N. Novgorod, Russia

[2]Kotelnikov Institute of Radio-Engineering and Electronics of RAS, Saratov Branch
38, Zelenaya str., 410019 Saratov, Russia

[3]Joint Institute for High Temperatures of RAS
13, Izhorskaya str., build 2, 125412 Moscow, Russia

[4]National Research Nuclear University «MEPhI»
31, Kashirskoye avenue, 115409 Moscow, Russia

E-mail: rrz@appl.sci-nnov.ru, isaevao@rambler.ru, ginzburg@appl.sci-nnov.ru, zotova@appl.sci-nnov.ru, sergeev@appl.sci-nnov.ru, rozhnevag@info.sgu.ru, karat@tarak.msk.su

Received 26.03.2018

Topic and aim. The dynamics of a double-resonator gyroklystron of the 93 GHz band with delayed feedback is studied. A comparative analysis of the dynamical regimes of amplifier generation obtained in the numerical experiment both on the basis of averaged equations and in the framework of direct numerical simulation by the «particle-in-cells» method using the KARAT code is carried out. **Method**. To identify the dynamical properties of system behavior we apply the spectrum of of statistical methods from the theory of chaos: the calculation of fractal dimensions, Lyapunov exponents, etc. To find the Lyapunov exponents we apply a method of estimating them from dynamical time series. This method is extremely convenient, since it requires only the single scalar time realization in a fixed in space point of spatially distributed system, for example, the amplitude of output radiation. Moreover, this method imitates the processing of the data that can be obtained in natural experiment. **Results**. The analysis of the time series obtained in numerical simulation showed the existence of hyper-chaotic regimes for both approaches to the modeling of gyroklystron. Such regimes correspond to attractors with a high correlation dimension and more than one positive Lyapunov exponents. It was found that mentioned hyperchaotic regimes occur, for example, with an increase in the transmission factor for the feedback loop. The multimode «strong» hyper-chaos arises from chaos resulting from the sequence of period doubling bifurcations of the periodic auto-modulation mode intensity of output radiation gyroklystron. **Discussion**. UHF chaotic and noise generators are extremely important for various technical applications. One can note, for example, radars and wideband communication. Thus, the production of multimode, chaotic and hyper-chaotic regimes of gyro-amplifiers generation is a priority branch of microwave electronics. Being proposed in this paper the mathematical modeling methods allow to detect complex regimes for gyroklystron. Being proposed in this paper the approaches to amplifier generations analysis can be applied in a physical experiment.

Key words: gyroklystron, delayed feedback, strong chaos.

DOI: 10.18500/0869-6632-2018-26-3-78-98

Reference: Pozental R.M., Isaeva O.V., Ginzburg N.S., Zotova I.V., Sergeev A.S., Rozhnev A.G., Tarakanov V.P. Automodulation and chaotic regimes of generation in a two-resonator gyroklystron with delayed feedback. *Izvestiya VUZ, Applied Nonlinear Dynamics,* 2018, vol. 26, no. 3, pp. 78–98. DOI: 10.18500/0869-6632-2018-26-3-78-98

Introduction

Gyroklystrons belong to one of the most well-studied type of gyroscopic amplifiers, characterized by a combination of high efficiency and gain [1–3]. Thus, in the range of 95 GHz in gyroklystrons, the output power is more than 300 kW [4], and in the 35 GHz range up to 12 MW [5]. At present, developments are to further increase the output power and operating frequency of these devices [6, 7]. At the same time, it is of some interest to obtain multifrequency, including chaotic, generation regimes, which can be achieved by introducing an external delayed feedback. Such a method is widely used in connection with ordinary klystrons, beginning with work [8] up to the present time [9, 10].

Under the approximation of the fixed longitudinal structure of the high-frequency field, the nonstationary modes of operation of gyroklistron with delayed feedback were investigated in [11, 12]. At the same time, as will be shown below, the model with self-consistent longitudinal structure proves to be more adequate for describing the developed chaotic regimes of generation. Within the framework of the model (see [13]), the space-time evolution of the field amplitude is described by a parabolic equation supplemented by the averaged equations of particle motion. This approach allows us to describe the amplification and generation of multifrequency broadband signals, taking into account the real dispersion of the electrodynamic system, the finiteness of the gain band, and the effects of nonlinear saturation.

1. Nonstationary self-consistent model of gyroklystron with diffraction input and radiation output

Let us consider the process of electron-wave interaction in gyroklystron, the input and output of radiation in which is carried out in a diffraction manner, which corresponds to a number of experimentally realized systems [14–16]. We assume the interaction space of a gyroklystron of length z_{out} to include the input and output resonators, as well as the drift space between them (Fig. 1).

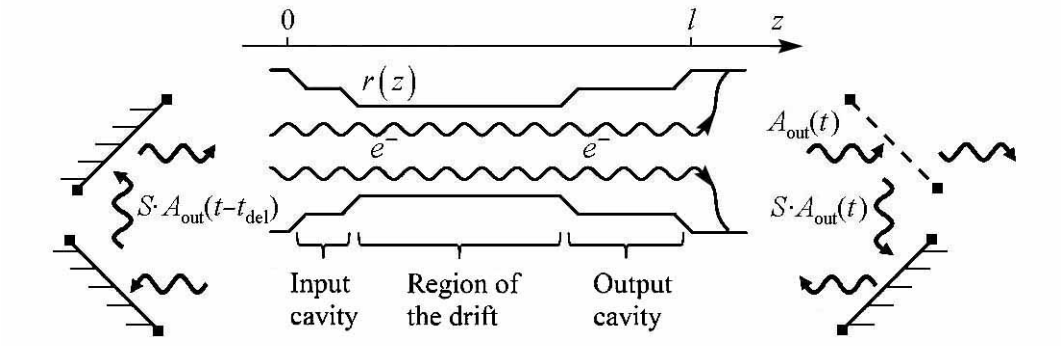

Fig. 1. Model of a two-cavity gyroklystron with diffraction input/output of radiation and a delayed feedback

The profile of the resonators and the drift space is described by the function $r(z)$. We will also assume that in both resonators the same TE_{mp} mode is excited at a frequency close to the cut-off frequency. In this case, the process of electron-wave interaction at the fundamental harmonic of cyclotron resonance can be described by the following system of equations [13]:

$$\begin{aligned} & i\frac{\partial^2 a}{\partial Z^2} + \frac{\partial a}{\partial \tau} + (\sigma(Z) + i\delta(Z))\, a = \frac{I_0}{2\pi}\int\limits_0^{2\pi} p d\theta_0, \\ & \frac{\partial p}{\partial Z} + \frac{g^2}{4}\frac{\partial p}{\partial \tau} + ip\left(\Delta_H - 1 + |p|^2\right) = -a. \end{aligned} \tag{1}$$

Here the following normalized variables are used:

$$\tau = \frac{\omega_c t \beta_{\perp 0}^4}{8\beta_{||0}^2}, \qquad Z = \frac{\beta_{||0}^2 \omega_c z}{2\beta_{||0} c}, \qquad p = \frac{(p_x + ip_y)e^{-i\omega_c t + i(m-1)\varphi}}{p_{\perp 0}},$$
$$a = \frac{eAJ_{m-1}(R_0\omega_c/c)}{mc\omega_c\gamma_0\beta_{\perp 0}^3}, \qquad I_0 = 16\frac{eI_b}{mc^3}\frac{\beta_{||0}}{\beta_{\perp 0}^6\gamma_0}\frac{J_{m-1}^2(R_0\omega_c/c)}{(\nu_p^2 - m^2)J_m^2(\nu_p)}.$$

I_b is the electron beam current, J_m is the Bessel function, ν_p is the p-th root of the equation $J_m'(\nu) = 0$, R_0 is the injection radius of the helical electron beam, $g = \beta_{\perp 0}/\beta_{||0}$ is the pitch factor, $V_{\perp 0} = \beta_{\perp 0} c$ and $V_{||0} = \beta_{||0} c$ c are the initial values of the transverse and longitudinal electron velocities, $\Delta_H = 2(\omega_c - \omega_H)/\omega_c\beta_{\perp 0}^2$ is the detuning parameter between the critical frequency of the working mode and the unperturbed gyrofrequency value. The $\delta(Z) = 8\beta_{||0}^2(\omega_c - \omega_c(Z))/\beta_{\perp 0}^4\omega_c$ describes the profile of the electrodynamic system, where $\omega_c(Z) = c\nu_p/r(Z)$.

We assume that at the entrance to the interaction space the electrons are uniformly distributed over the phases of cyclotron rotation $p(Z = 0) = \exp(i\theta_0)$, $\theta_0 = [0, 2\pi)$. At the output of the system in the section $Z = L$, $L = \beta_{\perp 0}^2\omega_c z_k/2\beta_{||0}c$ is the normalized length of the resonator, a radiative boundary condition is set [17]

$$a(L,\tau) + \frac{1}{\sqrt{\pi i}}\int\limits_0^{\tau}\frac{1}{\sqrt{\tau - \tau'}}\frac{\partial a(L,\tau)}{\partial Z}d\tau' = 0. \tag{2}$$

In the section $Z = 0$, a modified boundary condition is used, taking into account the arrival of the initial signal F (see [18])

$$a(0,\tau) - \frac{1}{\sqrt{\pi i}}\int\limits_0^{\tau}\frac{1}{\sqrt{\tau - \tau'}}\frac{\partial a(0,\tau)}{\partial Z}d\tau' = 2F(0,\tau). \tag{3}$$

Based on the developed model, we investigate the dynamics of two-cavity gyroklystron with an operating frequency of 93 GHz, which was experimentally investigated in [4]. We assume that a helical electron beam with a pitch factor of 1.3, an energy of 70 keV and a current of 15 A interacts with the mode TE_{02} in the input and output resonators at the fundamental harmonic of the gyrofrequency.

We assume that the feedback is realized by supplying a part of the radiation with a transmission coefficient S and a delay time $t_{\rm del}$ from the amplifier output to its input. In this case, the signal on the right-hand side of the boundary condition (3) can be represented in the form

$$F(0,\tau),= S\cdot a(Z_{\rm out},\tau-T), \tag{4}$$

where $T=\omega_c t_{\rm del}\beta_{\perp 0}^4/8\beta_{||0}^2$ is the normalized delay time. In the subsequent simulation, the propagation time of the signal along the feedback circuit T was chosen from the following considerations. As is known, in circuits based on low-power microwave amplifiers feedback circuits with delay times of hundreds of nanoseconds based on acoustic [19] or electro-optical [20] delay lines can be realized. At the same time, in instruments with a power level of tens or more kilowatts, to which the investigated gyroklystron of the 3 mm range belongs, it is possible to calculate only the delay lines of the waveguide type. In this case, the characteristic delay times are determined by the time at which the wave travels a distance comparable to the physical length of the amplifier. For this reason, the normalized delay value $T=20$, corresponding to the transmission of the signal along the feedback loop of about 50 cm in length, was used in the simulation.

2. Dynamics of gyroklystron with delayed feedback

The simulation shows that the generator self-excitation occurs at $S=0.05$. With increasing S up to values of $S\approx 1$, the lasing regimes remain stationary, which can be explained by a narrow band of gyroklystron gain, which for a relatively short delay time $T=20$ turns out to be less than the distance between the longitudinal modes. The frequencies of the longitudinal modes are determined in the first approximation by the expression

$$\omega_n \approx \frac{2\pi n}{t_{\rm del}+t_{\rm trans}}, \tag{5}$$

where n is the mode number, $t_{\rm trans}=z_{\rm out}/\nu_{||}$ is the time of flight of electrons through the interaction space of gyroklystron. With the chosen parameters, the frequency difference between adjacent longitudinal modes $(\omega_n-\omega_{n-1})$ is of the order of 500 MHz. A considerable increase in the width of the gyroklystron amplification band can be achieved by reducing the quality factor of the output resonator to values close to the minimum diffraction Q, $Q\approx Q_{min}\approx 4\pi(l/\lambda)^2$, where l is the length of the output cavity, λ is the operating wavelength [21]. As a result, the full gain band is expanded to values of the order of 5 GHz (Figure 2, curve 2), so that in the gain band there are about ten longitudinal modes of the ring resonator.

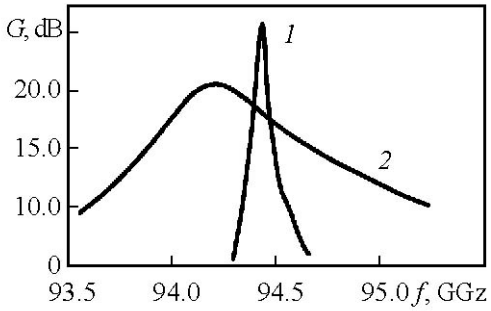

Fig. 2. The gyroklistron gain band: *1* – output resonator with the optimal quality factor; *2* – output resonator with a reduced quality factor

In a configuration with a reduced quality factor of the output resonator with a transmission coefficient $S\approx 0.52$, periodic self-modulation appears in the system (Fig. 3, *a*). In this case, the so-called amplitude scenario [22] is realized, when the period of self-modulation is close

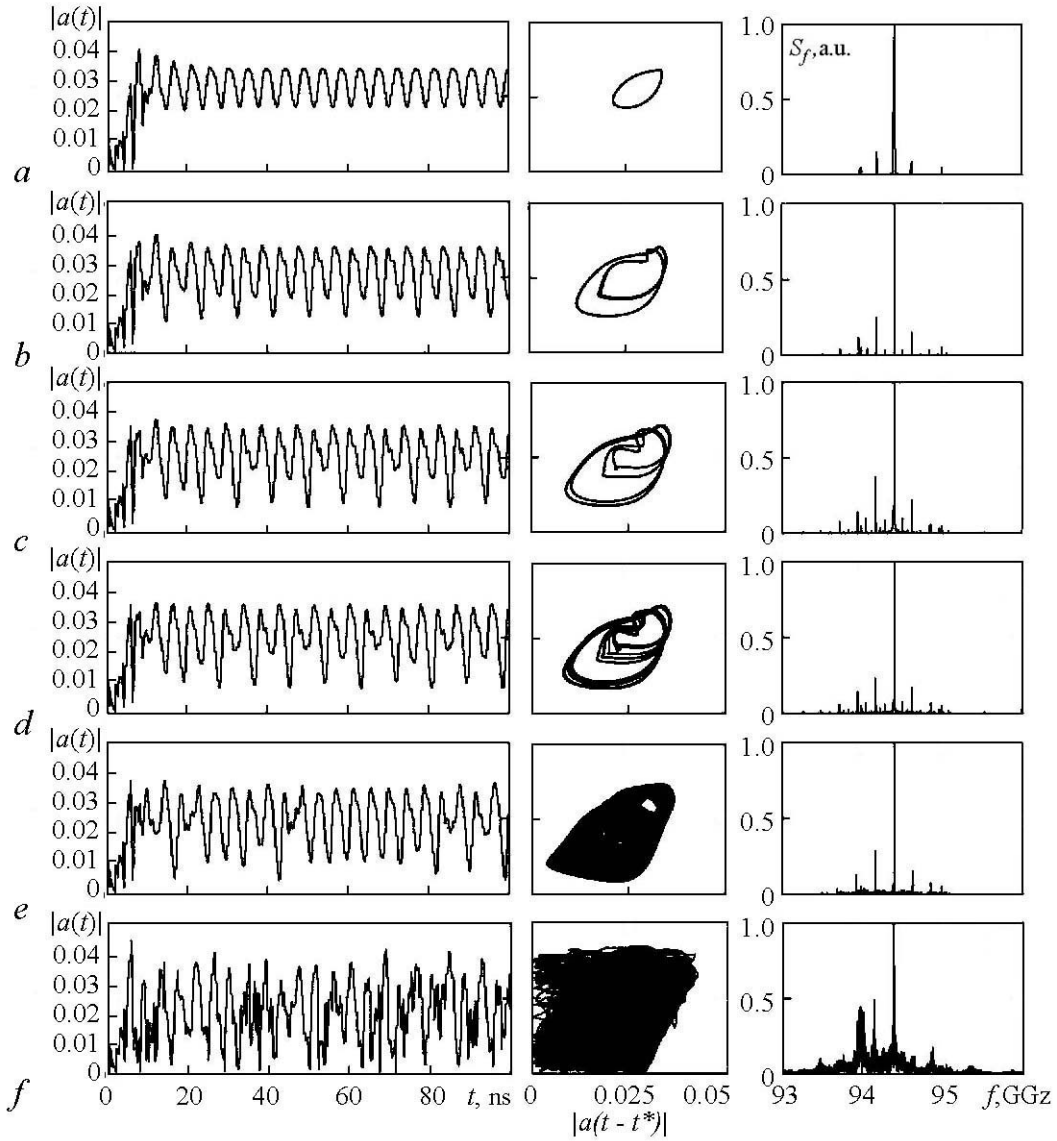

Fig. 3. Time series of the amplitude of output radiation of the gyroklystron with feedback (left), phase portrait (center) and the spectrum of the output radiation (right) for the different values of the transmission coefficient S: *a* – 0.56, *b* – 0.62, *c* – 0.64, *d* – 0.644, *e* – 0.67, *f* – 0.8. The value of $t^* \approx 0.6$ ns

to twice the transit time of the signal along the feedback loop. Accordingly, the self-modulation frequency ω_{AM}, which is about 216 MHz, is approximately equal to half the distance between the intrinsic longitudinal modes $(\omega_n - \omega_{n-1})/2 \approx$ ≈ 250 MHz. With increasing transmission coefficient in the interval $S = 0.53 - 0.64$, a sequence of several period-doubling bifurcations is observed (Fig. 3, *b*–*d*), which is also characteristic for the amplitude scenario, and then for $S \approx 0.65$ – transition to chaotic self-modulation (Fig. 3, *e*). The generation spectrum in this case is a set of isolated spectral lines with the frequencies 93.7, 93.93, 94.16, 94.39 and 94.64 GHz and the noise pedestal at the level of -40 dB. It must be noted that such a mechanism transition to chaos as a whole is characteristic for systems with delayed feedback [23].

With a further increase in the transmission coefficient in the range up to $S \approx$ ≈ 0.76, irregular generation regimes continue to exist, alternating with sufficiently wide windows of periodic self-modulation. This alternation of generation regimes is also characteristic of the classical klystron model with a delayed coupling, which was demonstrated in [24]. An even larger increase in the transmission coefficient in the distributed model of gyroklystron (1) leads to the realization of the «developed» chaos regimes, in which there are no large-scale structures on the phase portrait (as shown in Fig. 3, *f*).

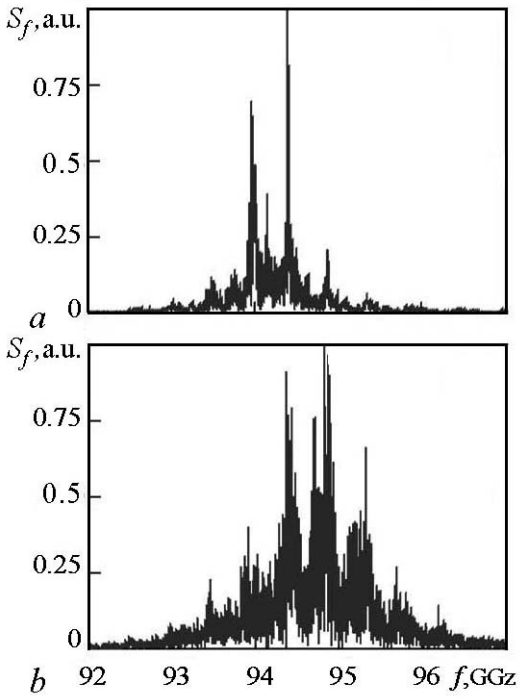

Fig. 4. The radiation spectrum of gyroklystron in the regime of stronge chaos: *a* – with normal length of the output cavity; *b* – in the case of a shortened output cavity

At the same time, the spectrum of the output signal changes significantly: the noise pedestal rises to a level (-15)–(-20) dB, and individual emission lines practically cease to be released. The width of the generation spectrum in gyroklystron with delayed feedback is limited by the band determined by the quality factor of the output resonator $\Delta f \approx f/Q$, where f is the central frequency of the radiation. Taking into account that $Q \approx Q_{min} \approx$ ≈ 130, the relative width of the radiation band even in chaotic regimes is less than 0.8% (Fig. 4, *a*). The average output power level is about 20 kW.

An increase in the width of the spectrum can be achieved by further reducing the quality factor of the output resonator by reducing its length. In order to compensate for the reduction in the gain, it is necessary to increase the length of the drift space. Calculations show that in this way the relative width of the emission spectrum can be almost three times increased to values of approximately 1.5% (Fig. 4, *b*). However, the average generation efficiency is reduced to about 3.5%.

3. PIC simulation of gyroklystron with delayed feedback

The simulation of electron-wave interaction was also carried out on the basis of the large-particle method. The simulation parameters corresponded to the characteristics of the experimental stand of the impulse gyroklystron of the 93 GHz band with the working mode TE_{02} on the first harmonic of the gyrofrequency [4]. Due to the axial symmetry of the interaction space, a 2.5-dimensional PIC version of the KARAT code was used for modeling [25, 26]. The geometry of the interaction space and the instantaneous position of the macroparticles are shown in Fig. 5. A helical electron beam with an energy of 70 keV, a current of 15 A, pitch factor 1.3 was injected into the resonator of a gyrotron with a radius of encroachment corresponding to the maximum of the coupling coefficient with the

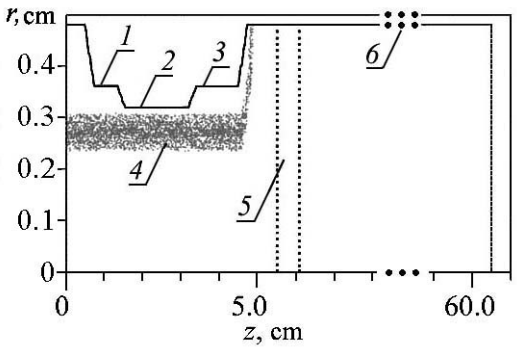

Fig. 5. Geometry of the interaction domain in PIC-simulation: *1* – input cavity, *2* – drift region, *3* – output resonator, *4* – electron beam, *5* – absorbing layer, *6* – waveguide delay line

working mode. After the termination of the interaction, the electrons were deposited on the wall of the electrodynamic system by introducing a decreasing portion of the magnetic field.

The delayed feedback line was created by adding a section of a homogeneous waveguide 55 cm long at the output of the system. To close the feedback loop, a special option of the KARAT code for generating cyclic boundary conditions was used. The transmission coefficient S was regulated by introducing into the waveguide delay line a layer with variable conductivity, the absorption coefficient of which was regulated by changing its geometric dimensions. The dimension of the counting grid was 40×2000 knots, the total number of macroparticles in the simulation reached $3.5 \cdot 10^4$. Control accounts with a tenfold increase in the number of particles showed no significant changes in the dynamics of the system.

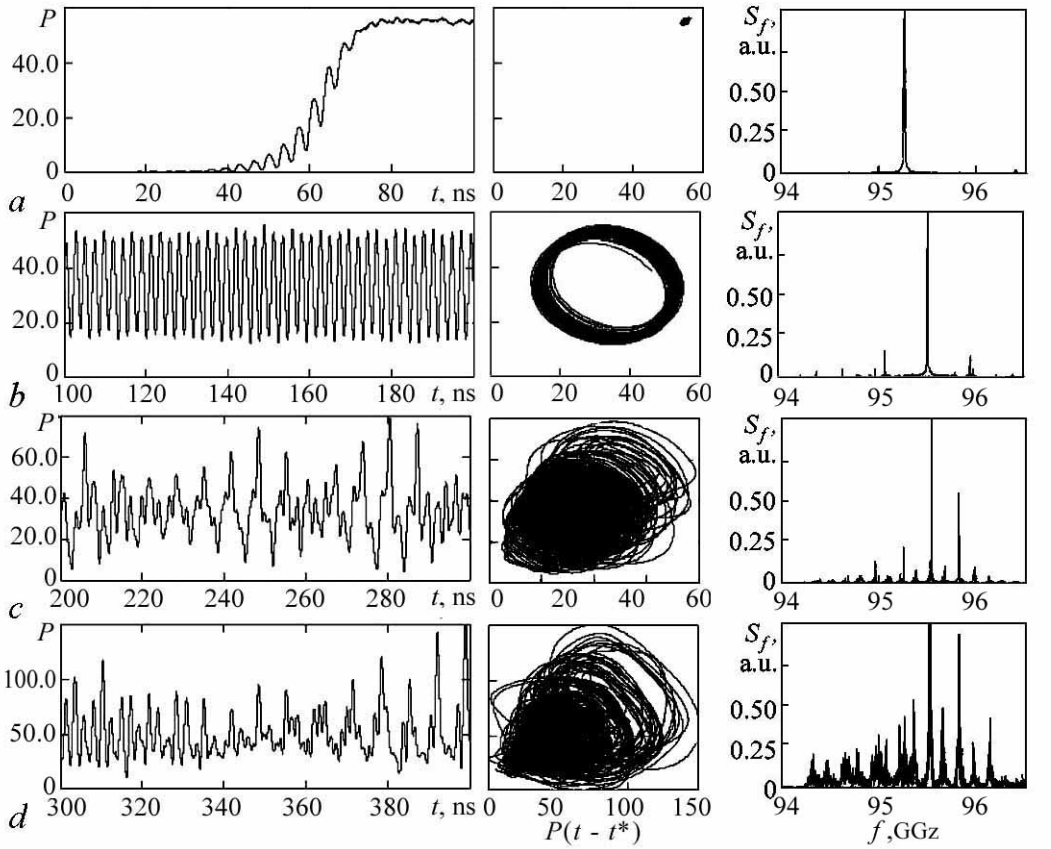

Fig. 6. The time evolution of the output radiation power of the gyroklystron (left), phase portrait (center) and the spectrum of the output radiation (right) for the different values of the transmission coefficient S: *a* – 0.22, *b* – 0.63, *c* – 0.7, *d* – 0.84. The value of $t^* \approx 0.6$ ns

The excitation of self-oscillations in this system occurred at $S > 0.2$ (Fig. 6, *a*). Periodic self-modulation occurred at $S \approx 0.63$ (Fig. 6, *b*), with the scenario corresponding to the frequency mechanism at which simultaneous excitation of several longitudinal modes of the ring resonator is confirmed, which is confirmed by the nearness of $\omega_{AM} \approx 514$ MHz to the calculated distance between the modes $\omega_n - \omega_{n-1} \approx 500$ MHz. With an increase in the transmission coefficient up to $S \approx 0.7$, a transition to the regime of chaotic lasing took place (Fig. 6, *c*), in which the spectrum consisted of isolated lines and a noise pedestal at a level of -50 dB. The discreteness of specifying the geometric parameters of the absorber did not allow us to set small changes in the depth parameter of the feedback, so in the simulation it was not possible to trace the details of the transition to chaotic lasing regimes. A further increase in the transmission coefficient led to a smearing of the spectral lines (Figure 6, *d*), which qualitatively corresponds to the behavior of the system in the framework of modeling the averaged equations (see Fig. 3, *f*). The average value of the useful output power in the mode of chaotic generation, calculated by the $P_{\text{out}} = (1 - S^2)P$, where P – power recorded at the output of gyroklystron, reached 10 kW. A smaller value of the average output power level can be explained by taking into account in PIC-simulation the initial spread of electrons over transverse velocities, which has a noticeable effect on the efficiency of energy exchange in gyroklystrons [27–29].

It is important to note that PIC-modeling clearly demonstrates the necessity of using models with a non-fixed field structure for describing chaotic regimes in gyroklystron with delayed feedback. This is confirmed by Fig. 7, which shows the spatio-temporal distribution of the longitudinal component of the magnetic field, averaged over the period of high-frequency oscillations, at a value of $S \approx 0.84$. It is seen that the longitudinal structure of the field varies considerably over time, which justifies the application of the approach considered in Section 2.

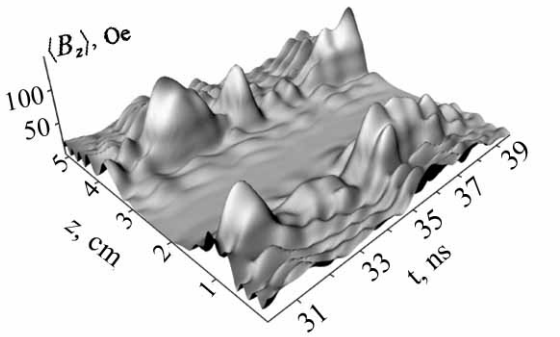

Fig. 7. The space-time distribution of the longitudinal component of the magnetic field, averaged over a period of high-frequency oscillations, with $S \approx 0.84$

4. Estimation of characteristics of chaotic regimes of gyroklystron operation

The regimes of developed chaos (Fig. 3, *f* and Fig. 6, *c, d*) detected during the numerical simulation of gyroklistron with delayed feedback require additional studies of their dynamic properties. Indeed, let us turn to Fig. 8. In Fig. 8, a is a bifurcation diagram for the distributed model (1). This is the dependence on the parameter S (transmission coefficient) of the values of the slow amplitude of the output radiation, which coincide in times that differ by the value of t^*. As can be seen, the crown of a bifurcation tree does not have pronounced windows for large S, which indicates a greater roughness of the attractors corresponding to it. One can compare a tree to a distribution diagram of the autocorrelation function as a function of the transmission coefficient, which varies within the same limits (Fig. 8, *b*). In the region of developed chaos, the function decays much more rapidly than for the chaotic regime that appeared immediately after the doubling

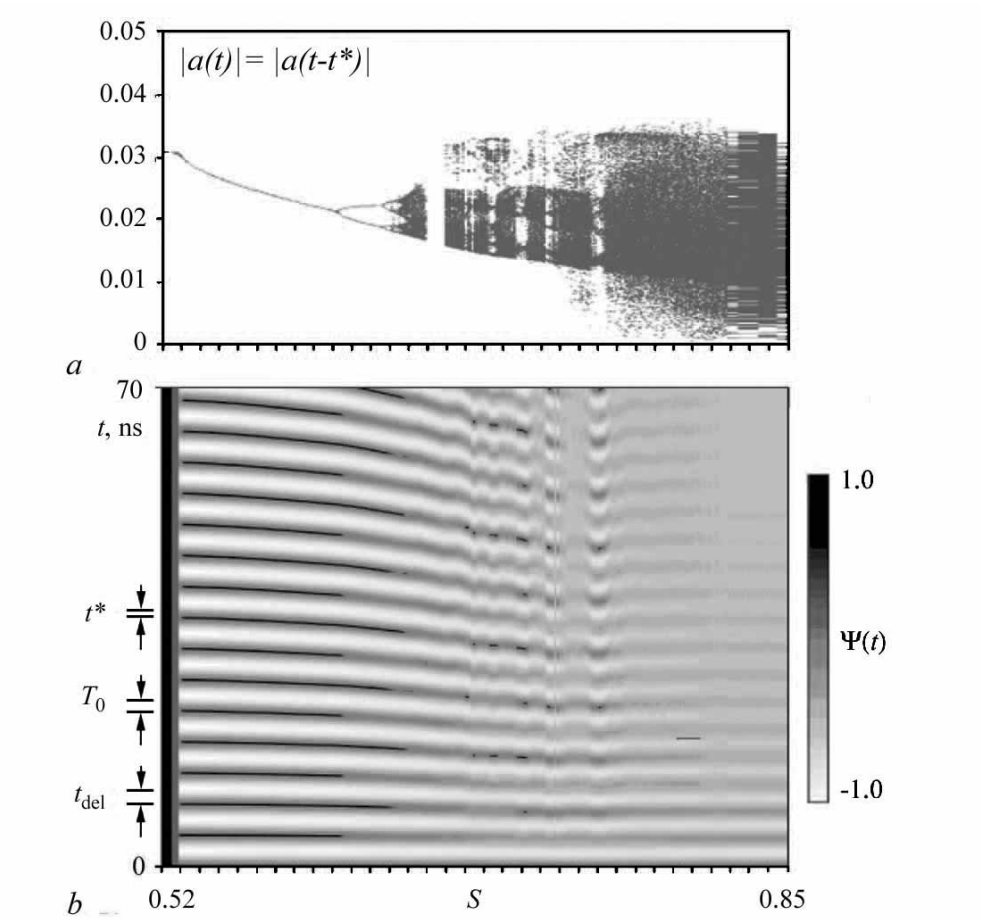

Fig. 8. The bifurcation diagram for the spatially distributed model (1) of the gyroklystron with the delayed feedback (*a*). The distribution of the autocorrelation functions depending on the transmission coefficient (*b*)

sequence. One of the reasons for these phenomena can be a qualitative change in the topology of the attractor with its transition to the class of hyperchaotic. To confirm this hypothesis, it is required to calculate the correlation dimension and, most importantly, the spectrum of Lyapunov exponents of the attractor [30–32].

Characteristic Lyapunov exponents have the meaning of the rates of exponential growth or decrease of the perturbation relative to the invariant phase trajectory in various directions. The spectrum of d indices is calculated as follows [30, 33, 34]

$$\Lambda_i = \lim_{t\to\infty} \Sigma_i(t), \quad \Sigma_i(t) = \frac{1}{MT_0} \sum_{m=1}^{M} \ln \left\| \mathbf{b}^{(T_0)}(t = mT_0)\mathbf{e}_i(t = mT_0) \right\|, \quad i = 1, 2, ..., d. \tag{6}$$

Here the value of d does not exceed the dimension of the phase space and will be defined below; $(\mathbf{e}_1, ..., \mathbf{e}_d)$ is the set of perturbation vectors; matrix $\mathbf{b}$ is a linear evolution operator. The perturbation vectors are taken to be orthogonal at the initial instant of time. To avoid their convergence to the single most unstable direction, they are orthogonalized after each calculation of the next contribution to the accumulating averaged sums Σ_i. The Gram-Schmidt orthogonalization constructs vectors in order of decreasing instability of the directions corresponding to them.

The spectrum of the Lyapunov exponents of the dynamic regimes of microwave devices was calculated earlier, for example, for a BWT [35, 36], a gyrotron [37, 38], a klystron [39]. In all cases, the Benettin algorithm was used [40, 41]. In this paper a different approach is applied. The Lyapunov exponents are calculated from the obtained numerical time series. At the same time, we used the more successful, in our opinion, comparison with the best-known [42–44] Sano-Savad technique [45], which saves machine time and is suitable for relatively short series [46]. At the same time, this approach is more accurate than the approximate Benettin algorithm, using «close» trajectories for estimating a linear operator whose exact calculation is difficult in systems of this type. In addition, the calculation of the characteristics of the output radiation from time series simulates the analysis of the results of the full-scale experiment. For more details on the advantages of the chosen method and the features of its application, see [47].

In Fig. 9, *a* shows the results of calculating the spectrum of Lyapunov exponents of a spatially distributed model of gyroklystron (1) The graphs of the dependence on the transmission coefficient of the five Lyapunov exponents confirm the occurrence of

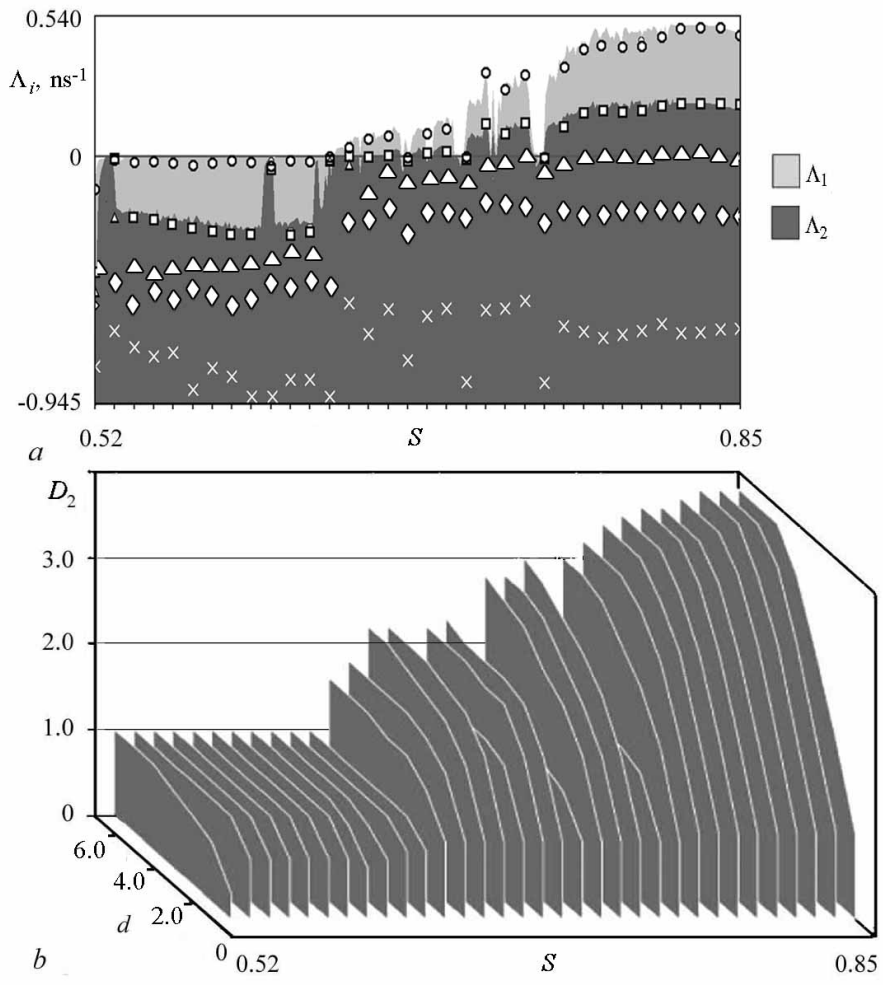

Fig. 9. For the slow amplitude model of gyroklystron the transmission coefficient dependences of the spectrum of five Lyapunov exponents ($i = 1$ – circles, 2 – squares, 3 – triangles, 4 – diamonds, 5 – asterisks) (*a*) and the distribution of correlation dimension D_2 on the reconstructed phase space dimension d (*b*)

hyperchaos at large S, namely, the two leading indicators become positive. In this case, it jumps and exceeds the value 3 and the correlation dimension (Fig. 9, *b*).

By correlation dimension is meant the value to which D_2 tends as the dimension d of the state vector a reconstructed by the delay method is a $\mathbf{a}(t) = (|a(t)|, |a(t-T_0)|, ..., |a(t-(d-1)T_0)|)$. In this case, D_2 has the meaning of the slope angle of the graph of the correlation integral constructed on the logarithmic scale $C(\delta) = \lim\limits_{t\to\infty} \frac{1}{t^2} \int_0^t \int_0^t \theta \times \times(\delta - \|\mathbf{a}(t') - \mathbf{a}(t'')\|)dt'dt''$ (here θ is the Heaviside step function). As T_0, the time for the autocorrelation function to decrease to zero (approximately 1ns) is used. The value $d = 5$, at which the value of D_2 stabilizes, served as an estimate of the dimension of the reconstructed phase space: an attractor can be embedded into it without self-intersections. Similar calculations were carried out for the time realizations obtained in the numerical simulation by the large-particle method. The results for the calculation of Lyapunov exponents and fractal dimensions (correlation D_2 and a well-matched Lyapunov D_λ) for several values of the transmission coefficient are given in Table. The Lyapunov dimension was defined as $D_\lambda = k + \sum_{i=1}^{k} \Lambda_i / |\Lambda_{k+1}|$, where k is the minimum number of older exponents whose sum is positive.

Table

Lyapunov exponents and fractal dimensions
of attractors obtained in PIC numerical simulation

S	Λ_1, ns^{-1}	Λ_2, ns^{-1}	Λ_3, ns^{-1}	Λ_4, ns^{-1}	Λ_5, ns^{-1}	D_2	D_λ
0.54	-0.028	-0.185	-0.237	-0.312	-0.431	0.0	0.0
0.63	0.066	0.000	-0.052	-0.161	-0.364	3.0	3.1
0.70	0.322	0.137	0.009	-0.099	-0.298	4.5	5.2
0.77	0.199	0.080	-0.009	-0.128	-0.355	4.1	4.4
0.84	0.237	0.095	-0.009	-0.118	-0.336	4.6	4.6
0.91	0.241	0.090	-0.009	-0.137	-0.331	4.4	4.6

An example of calculating the averaged sums accumulating to characteristic exponents Σ_i is presented for this case in Fig. 10, *a*. The sums quickly converge. Local Lyapunov exponents averaged over a relatively narrow time window along the phase trajectory fluctuate in their vicinity and characterize the development of instability along it. The values of the correlation dimension D2 reach saturation at $d = 5$ and assume a value greater than 4 (see Fig. 10, *b*).

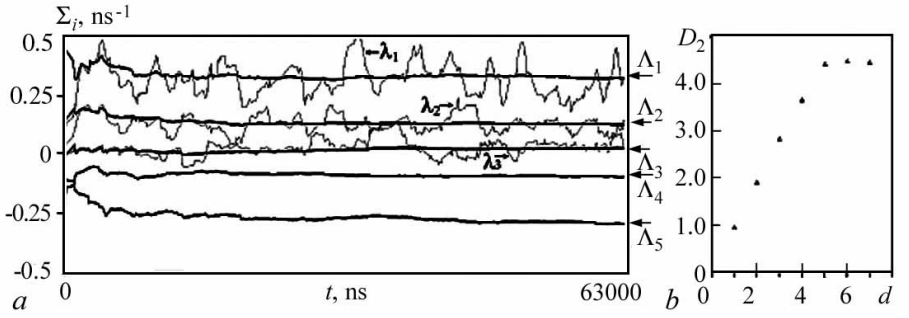

Fig. 10. The characteristics of the hyperchaotic attractor obtained in the PIC simulation of gyroklystron with $S = 0.70$. The averaged accumulated sums, converging to the five senior Lyapunov exponents, and the three senior local exponents (*a*). The correlation dimension vs the dimension of the phase space (*b*)

The results of the analysis of the temporal realizations of the intensity of the output radiation in PIC modeling also confirm the presence of hyperchaos in the dynamics of gyroklystron: two positive Lyapunov exponents and a high correlation dimension occur at $S = 0.91$, 0.84, 0.77 and 0.7. Calculations for the case $S = 0.54$ show the absence of auto-modulation. The not too large positive value of one of Lyapunov's exponents at $S = 0.63$ can be to some extent due to the influence of numerical error in the calculation of realizations and, at the same time, indicates the emerging chaos.

5. Conclusions

The non-stationary distributed model of gyroklystron with delayed feedback, in contrast to the previously used models [48, 49] allows to study the dynamics of the system for arbitrary relations between the resonator Q-factors, the delay time of the signal, and the transmission coefficient of the feedback loop. This allows us to adequately describe the regimes of developed chaos, characterized, in particular, by significant changes in the longitudinal structure of the electromagnetic field.

It should be noted that a number of studies are currently underway to investigate noise sources in the millimeter range on the basis of helical gyro-TWT with delayed feedback [48] «nanowirts» [49] and gyrotrons [50]. Given the current prospects for promoting gyroklystron in the region of large operating frequencies and capacities, understanding the characteristics of chaotic regimes is a very urgent task.

References

1. Andronov A.A., Flyagin V.A., Gaponov A.V., Gol'denberg A.L., Petelin M.I., Usov V.G., Yulpatov V.K. The gyrotron: High-power source of millimetre and submillimetre waves. *Infrared Phys.*, 1978, vol. 18, no. 5–6, pp. 385–393.
2. Nusinovich G.S. Introduction to the Physics of Gyrotrons. Baltimore: J. Hopkins Univ. Press, 2004, 341 p.
3. Thumm M. State-of-the-art of high power gyro-devices and free electron masers, Update 2016. *KIT Scientific Reports*, 2017, Band-Nr, 7735.
4. Zasypkin E.V., Gachev I.G., Antakov I.I. Experimental study of a W-band gyroklystron amplifier operated in the high order TE_{021} cavity mode. *Radiophys. Quant. El.*, 2012, vol. 55, no. 5, pp. 309–317.
5. Zaitsev N.I., Gvozdev A.K., Zapevalov S.A., Kuzikov S.V., Manuilov V.N., Moiseev M.A., Plotkin M.E. Experimental study of a multimegawatt pulsed gyroklystron. *Journal of Communications Technology and Electronics*, 2014, vol. 59, no. 2, pp. 164–168.
6. Zaitsev N.I., Abubakirov E.B., Guznov Yu.M., Denisov G.G., Zavolskii N.A., Zapevalov V.E., Zapevalov S.A., Plankin O.P., Rozental R.M., Sedov A S., Semenov E.S., Chirkov A.V., Shevchenko A.S. *Book of abstracts of 25th Int. Crimean Conf. «UHF-technics and Telecommunication Technologies»*, Sevastopol, September 6–12 2015, pp. 781–782.
7. Swati M.V., Chauhan M.S., Jain P.K. Design methodology and beam-wave interaction study of a second-harmonic D-band gyroklystron amplifier. *IEEE Trans. Plasma Sci.*, 2016, vol. 44, no. 11, pp. 2844–2851.

8. Kuznetsov S.P., Perelman A.Yu., Trubetskov D.I. *Technical Physics,* 1983, vol. 53, no. 1, pp. 163–166.
9. Grishin S.V., Dmitriev B.S., Zharkov Y.D., Skorohodov V.N., Sharaevskii Y.P. Generation of chaotic microwave pulses in a ring system based on a klystron power amplifier and a nonlinear delay line on magnetostatic waves. *Technical Physics Letters*, 2010, vol. 36, iss. 2, pp. 76–79.
10. Emelyanov V.V., Girevoy R.A., Yakovlev A.V., Ryskin N.M. Time-domain particle-in-cell modeling of delayed feedback klystron oscillators. *IEEE Trans. Electron. Dev.*, 2014, vol. 61, no. 6, pp. 1842–1847.
11. Ergakov V.S., Moiseev M.A. Two-cavity oscillator with external delay feedback. *Radiotekhnica i Electronica*, 1986, vol. 31, iss. 5, pp. 962–967 (in Russian).
12. Afanasieva V.V., Lazerson A.G. Chaotic dynamics of two-cavity clystron oscillators with delayed feedback. *Izvestiya VUZ. Applied Nonlinear Dynamics*, 1995, vol. 3, no. 5, pp. 88–99. (in Russian).
13. Ginzburg N.S., Rozental R.M., Sergeev A.S., Zotova I.V. Time-domain model of gyroklystrons with diffraction power input and output. *Physics of Plasmas*, 2016, vol. 23, 033108–033112.
14. Zasypkin E.V., Moiseev M.A., Gachev I.G., Antakov I.I. Study of high-power Ka-band second-harmonic gyroklystron amplifier. *IEEE Trans. Plasma Sci*., 1996, vol. 24, no. 3, pp. 666–670.
15. Tolkachev A.A., Levitan B.A., Solovjev G.K., Veytsel V.V., Farber V.E. A megawatt power millimeter-wave phased-array radar. *IEEE Aerospace and Electronic Systems Magazine*, 2000, vol. 15, pp. 25–31.
16. Antakov I.I., Gachev I.G., Zasypkin E.V. Experimental studies of a gyroklystron operating in the field of a permanent magnet. *Radiophys. Quant. El.*, 2011, vol. 54, no. 3, pp. 166–173.
17. Ginzburg N.S., Zavolsky N.A., Nusinovich G.S. Theory of non-stationary processes in gyrotrons with low-Q resonators. *Int. J. Electron.*, 1986, vol. 61, pp. 881–894.
18. Ginzburg N.S., Sergeev A.S., Zotova I.V. Time-domain self-consistent theory of frequency-locking regimes in gyrotrons with low-Q resonators. *Phys. Plasmas*, 2015, vol. 22, 033101–033105.
19. Katz V.A. Appearance of chaos and its evolution in a distributed oscillator with delay (experiment). *Radiophys. Quant. El.*, 1985, vol. 28, no. 2, pp. 107–119.
20. Ustinov A.B., Kondrashov A.V., Kalinikos B.A. A microwave photonic generator of chaotic and noise signals. *Technical Physics Letters*, 2016, vol.42, no.4, pp.403–406.
21. Vlasov S.N., Zhislin G.M., Orlova I.M., Petelin M.I., Rogacheva G.G. Irregular waveguides as open resonators. *Radiophys. Quant. El.*, 1969, vol.12, no.8, pp.972–978.
22. Ryskin N.M. Study of the nonlinear dynamics of a traveling-wave-tube oscillator with delayed feedback. *Radiophysics and Quantum Electronics*, 2004, vol. 47, no. 2, pp. 116–128.
23. Kuznetsov S.P. Complex dynamics of oscillators with delayed feedback (review). *Radiophys. Quant. El.*, 1982, vol. 25, no. 12, pp. 996–1009.
24. Dmitrieva T.V., Ryskin N.M., Titov V.N., Shigaev A.M. Complex dynamics of

the simple models of distributed electron-wave systems. *Izvestiya VUZ, Applied Nonlinear Dynamics*, 1999, vol. 7, no. 6, pp. 66–81 (in Russian).

25. Tarakanov V.P. The Universal Electromagnetic Code KARAT. Math. Modeling. Problems and Results. Moscow: Nauka, 2003, 456 p. (in Russian).
26. Tarakanov V.P. Code KARAT in simulations of power microwave sources including Cherenkov plasma devices, vircators, orotron, E-fieldsensor, calorimeter etc. *EPJ Web of Conferences*, 2017, vol. 149, 04024.
27. Ergakov V.S., Moiseev M.A. *Electronnaya Tekhnica, Ser I, Electronica SVCH*, 1977, no. 5, pp. 9–15 (in Russian).
28. Ergakov V.S., Moiseev M.A., Erm R.E. *Electronnaya Tekhnica. Ser I. Electronica SVCH*, 1980, no. 4, pp. 29–37 (in Russian).
29. Zasypkin E.V., Moiseev M.A. Efficiency enhancement in gyroklystrons with a nonuniform static magnetic field. *Radiophys. Quant. El.*, 1994, vol.37, no.10, pp.853–862.
30. Kuznetsov S.P. Dynamical Chaos. Moscow: Fizmatlit, 2006. 356 p. (in Russian).
31. Bezruchko B.P., Smirnov D.A. Extracting Knowledge from Time Series. An Introduction to Nonlinear Empirical Modeling. Heidelberg–Dordrecht–London–New York: Springer, 2010. 420 p.
32. Bradley E., Kantz H. Nonlinear time-series analysis revisited. *Chaos,* 2015, vol. 25, 097610–097619.
33. Lyapunov A.M. General Problem of the Motion Stability. Moscow–Leningrad: GITTL, 1950, 472 p. (in Russian).
34. Eckmann J.-P., Ruelle D. Fundamental limitations for estimating dimensions and Lyapunov exponents in dynamical systems. *Physica D*, 1992, vol. 56, pp. 185–187.
35. Bezruchko B.P., Bulgakova L.V., Kuznetsov S.P., Trubetskov D.I. *Radiotekhnica i Electronica*, 1983, vol. 28, no. 6, pp. 1136–1139 (in Russian).
36. Kuznetsov S.P., Trubetskov D.I. Chaos and hyperchaos in a backward-wave oscillator. *Radiophys. Quant. El.*, 2004, vol. 47, no. 5–6, pp. 341–355.
37. Blokhina E.V., Rozhnev A.G. Chaos and hyperchaos in a gyrotron. *Radiophysics and Quantum Electronics*, 2006, vol. 49, no. 10, pp. 799–810.
38. Blokhina E.V., Kuznetsov S.P., Rozhnev A.G. High-dimensional chaos in a gyrotron. *IEEE Trans. Electron. Dev.*, 2007, vol. 54, no. 2, pp. 188–193.
39. Balyakin A.A., Ryskin N.M. Peculiarities of calculation of the Lyapunov exponents set in distributed self-oscillated systems with delayed feedback. *Izv. VUZ. Applied Nonlinear Dynamics*, 2007, vol. 15, no. 6, pp. 3–21 (in Russian).
40. Benettin G., Galgani L., Giorgilli A., Strelcyn J.-M. Lyapunov characteristic exponents for smooth dynamical systems and for Hamiltonian systems; A method for computing all of them. Part 1: Theory. *Meccanica*, 1980, vol. 15, pp. 9–20.
41. Benettin G., Galgani L., Giorgilli A., Strelcyn J.-M. Lyapunov characteristic exponents for smooth dynamical systems and for Hamiltonian systems; A method for computing all of them. Part 2: Numerical application. *Meccanica*, 1980, vol. 15, pp. 21–30.
42. Wolf A., J.Swift B., Swinney H.L., Vastano J.A. Determining Lyapunov exponents from a time series. *Physica D*, 1985, vol. 16, pp. 285–317.

43. Eckmann J.-P., Kamphorst S.O., Ruelle D., Gilberto D. Lyapunov exponents from a time series. *Phys. Rev. A*, 1986, vol. 34, pp. 4971–4979.
44. Brown R., Bryant P., Abarbanel H.D.I. Computing the Lyapunov spectrum of a dynamical system from an observed time series. *Phys. Rev. A*, 1991, vol. 43, pp. 2787–2806.
45. Sano M., Sawada Y. Measurement of the Lyapunov spectrum from a chaotic time series. *Phys. Rev. Lett.*, 1985, vol. 55, pp. 1082–1085.
46. Zeng X., Eykholt R., Pielke R.A. Estimating the Lyapunov exponent spectrum from short time series of low precision. *Phys. Rev. Lett.*, 1991, vol. 66, pp. 3229–3232.
47. Rozental R.M., Isaeva O.B., Ginzburg N.S., Zotova I.V., Sergeev A.S., Rozhnev A.G. Characteristics of chaotic regimes in a space-distributed gyroklystron model with delayed feedback. *Rus. J. Nonlin. Dyn.*, 2018, no. 2 (in press).
48. Ginzburg N.S., Rozental R.M., Sergeev A.S., Zotova I.V. Generation of ultrashort microwave pulses in the sub-THz and THz range based on the cyclotron superradiance effect. *Technical Physics Letters*, 2017, vol. 43, no. 9, pp. 831–834.
49. Frolov N.S., Kurkin S.A., Koronovskii A.A., Hramov A.E. Nonlinear dynamics and bifurcation mechanisms in intense electron beam with virtual cathode. *Phys. Lett. A,* 2017, vol. 381, no. 28, pp. 2250–2255.
50. Rozental R.M., Ginzburg N.S., Sergeev A.S., Zotova I.V., Fedotov A.E., Tarakanov V.P. Gyrotron generation of broadband chaotic radiation under overlapping of high- and low-frequency resonances. *Technical Physics*, 2017, vol. 62, no. 10, pp. 1562–1568.